Chiang Mai J. Sci. 2016; 43(2) : 393-401
http://epg.science.cmu.ac.th/ejournal/
Contributed Paper

Semi-Solid State Joining of SSM Aluminum Alloys Using Brazing ZA27

Thammanoon Phonin[a] , Prapas Muangjunburee*[b]

[a] Department of Mining and Materials Engineering, Faculty of Engineering, Prince of Songkla University, Hatyai, Songkhla 90112, Thailand.

*Author for correspondence; e-mail: prapas.m@psu.ac.th

Received: 15 September 2015
Accepted: 14 November 2015

ABSTRACT

Semi-solid state joining of SSM A356 aluminum alloy under normal atmosphere using ZA27 as a filler was investigated. Localized semi-solid pool of ZA27 filler was created by an induction heating coil for butt joint of SSM A356. Then a stirrer was applied into the weld seam to stir the filler. The accurate control of semi-solid temperature during joining was measured. The effect of welding speed on physical and mechanical properties, macrostructure and microstructure was studied. The results showed that the weld microstructure was rosette globular structure. In addition, voids were found at the seam. The interface between base metal and filler exhibited sound bond. A decrease in welding speed resulted in a reduction in a number of voids presented in the structure. The best tensile strength and micro hardness of the joints were obtained from the optimum condition using rotation speed at 1,750 rpm and welding speed at 15 mm/min.

Keywords: Semi-Solid State Joining, SSM A356 Aluminum Alloy, ZA27

1. INTRODUCTION

In these modern times, demand of aluminum alloy casting parts in automotive manufactures is very high, such as suspension system, transmissions and engine parts as well as other industries in order to reduce weight and power consumption [1]. Thus there are competing technologies in aluminum casting widely. To increase the efficiency and quality, the latest technology, that has the potential, is a process of rheocasting. About 9-10 years ago, a group of researchers developed a new rheocasting technique called GISS (Gas Induced Semi-Solid) [2]. Recently, GISS Process, has been developed as a new semi-solid metal processing to create semi-solid slurry with the benefits of both higher efficiency and lower cost as well as providing the globular microstructure of the base metal [3].

The joining process of SSM aluminum alloys has been performed using various techniques. Liquid state joining processes lead to the formation of defects such as porosity in the weld, whereas solid state joining processes cause change in microstructure of the weld [4-5]. And recently, semi-solid state

joining process has been combined with the foundation of SSM processing. The semi-solid state joining processes of zinc AG40A and A356 aluminum alloy were studied; a localized semi-solid pool of the materials was developed by a gas heating system and stirring in which the joints obtained were globular microstructure [6-7]. The semi-solid state joining of SiC_p/A356 composites by semi-solid stirring brazing was developed. A localized semi-solid pool of the brazing was created and stirred [8-9]. Although welding of aluminum alloy casting by semi-solid state joining is a very new technology, this technique is probably more appropriate than solid and liquid state weldings. The purpose of this research is to improve the metallurgical and mechanical properties of semi-solid state joining of SSM aluminum alloys using ZA27 brazing. The influence of welding speed on physical and mechanical properties, macro-structure and microstructure was investigated.

2. EXPERIMENTAL

SSM A356 Aluminum alloys were obtained via squeeze casting GISS process and their composition is shown in Table 1. The filler metal used was Zn-Al alloy which its chemical composition is illustrated in Table 2. Its solidus-liquidus temperature was in a range of 440-490 °C. The base and the filler metals were plated in shape with the dimensions of $4 \times 40 \times 100$ mm^3 and $4 \times 3.5 \times 100$ mm^3, respectively. The specimens were fixed on a moving table. Tools and equipment used for the semi-solid state joining is shown in Figure 1. The filler metal was positioned between the faying surfaces of the base metal as demonstrated in Figure 2. Before joining, the filler was heated to a semi-solid temperature of 450°C, using an induction heating coil, and kept for 7 minutes. A thermocouple was used to measure the temperature and the accuracy of the temperature control was ±10°C.

Then a stirrer with 3.5 mm in diameter and 2° vertical angle was used to homogeneously stir the semi-solid filler. The welding speeds were varied: 15, 25, 40 and 70 mm/min. The stirrer rotation speed was fixed at 1750 rpm. After joining, the sample was cooled down to room temperature under a normal atmosphere.

Table 1. Chemical composition of the aluminum alloys (weight %) [8].

Si	Cu	Mg	Fe	Zn	Mn	Ti	Ni	Al
7.130	0.041	0.247	0.119	0.006	0.006	0.154	0.004	Bal.

Table 2. Chemical composition of the filler metal (weight %) [11].

Materials	Aluminum	Copper	Magnesium	Iron	Lead	Nickel
ZA27	25.0-28.0	2.0-2.5	0.01-0.02	0.075max	0.006max	Remainder

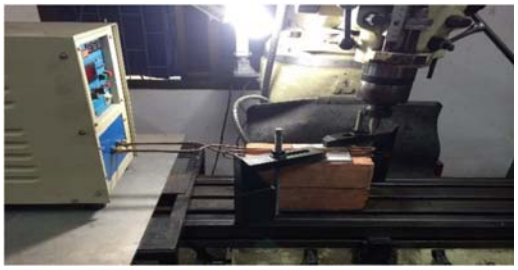

(a)

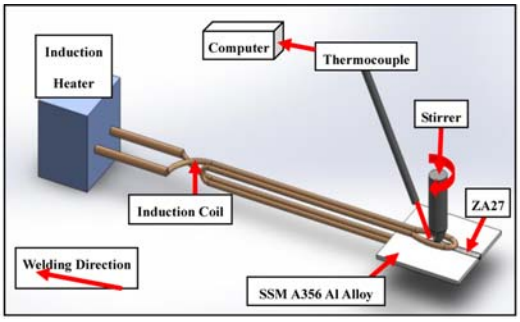

(b)

Figure 1. Semi-solid state joining equipment (**a**) the photograph with (**b**) the schematic diagram.

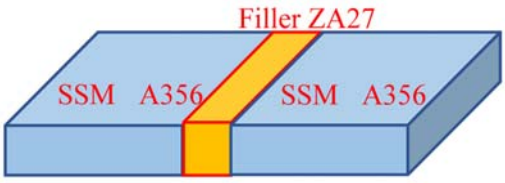

Figure 2. Schematic of the semi-solid stirring process.

The cross sections of bonded joints were prepared by standard grinding and polishing techniques for metallographic analysis. The sample was etched with 2% Nital and the microstructure was examined using optical microscope and scanning electron microscope.

Tensile strength of the bonded joints was measured based on the ASTM-E8M standard using a Hounsfield model H100KS universal testing machine with a cross head speed of 1.002 mm/min. The tensile test specimens were prepared with 6 mm in width, 4 mm in thickness and 25 mm in length.

Vickers hardness was measured at the area of base metal, interface and filler using Vickers indenter with 98.07 N load for 10 s.

3. RESULTS AND DISCUSSION

3.1 Macrostructure and Microstructure of The Joints

The top surface appearances of the semi-solid state joining samples under various joining conditions are shown in Figure 3. When the welding speed rate was low, smooth surface and pits were found on the top surface of the weld metal zone (see Figure 3a-b). However, with increasing the welding speed, the top surface of the weld metal zone changed to coarse surface and larger pits (see Figure 3c-d). Increase in welding speed can lead to less stirring time and cause squeezed out and more pits throughout the weld surface.

Macrostructure of the joints was obtained using low magnification of the optical microscope and displayed in Figure 4. At low welding speed (15 mm/min), it was found that the filler metal was squeezed out. This phenomenon, however, was not observed in other higher welding speeds. In addition, it depicts clearly the scattered voids in brazed ZA-27 located near the top of the surface.

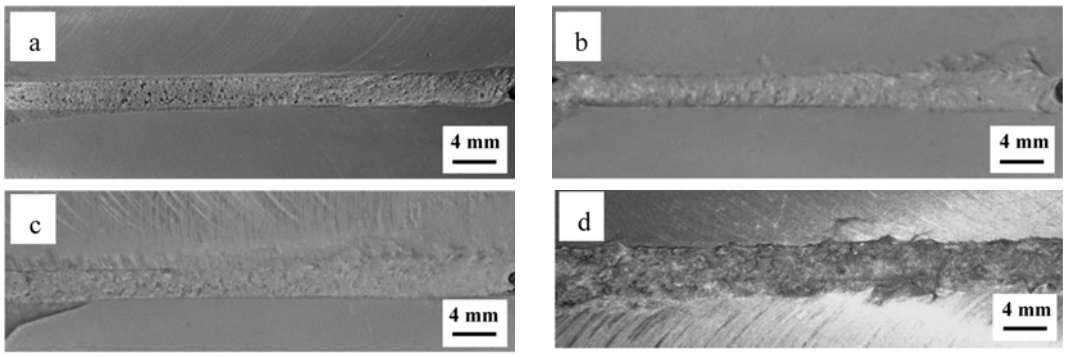

Figure 3. Appearances of the top surfaces of the joints obtained from various welding speed of (a) 15 mm/min, (b) 25 mm/min, (c) 40 mm/min and (d) 70 mm/min.

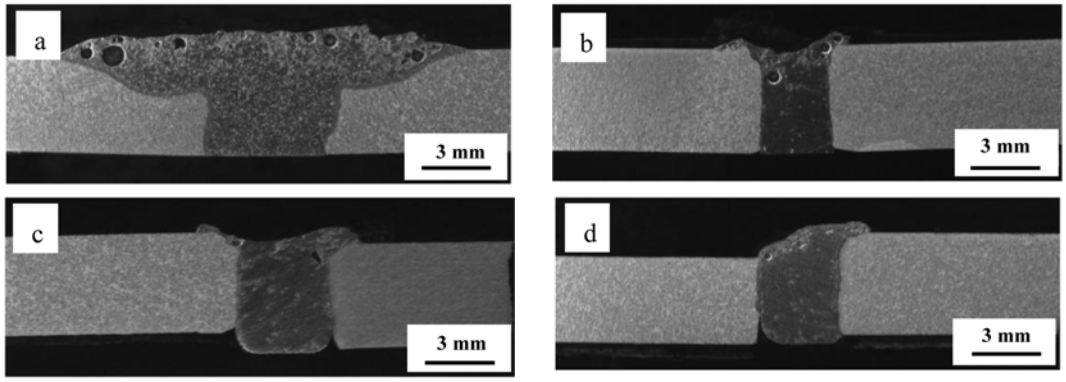

Figure 4. Macrostructure of the joints: (a) 15 mm/min, (b) 25 mm/min, (c) 40 mm/min and (d) 70 mm/min.

Figure 5 shows microstructure of the joint interface for both retreating and advancing sides. The white band at the interface was observed clearly. When a greater welding speed was applied, a large number of voids appeared along interface adjacent to the filler. (see Figure 5b-d). Therefore, the increased welding speed led to an increase in a number of voids along the interface. It is indicated that an increase in welding speed causes the interaction between the filler metal and the base metal. This is because when the welding speed is low, it allows sufficient time for the slurry metal to fill up the voids.

Figure 6 shows microstructure of the joints (ZA27) welded in semi-solid state joining. The ZA27 exhibited the globular microstructure called rossett-like. The eutectic phase is located between the globules. All welding speeds revealed similar size of the globular microstructure. Such microstructure of the joints confirms the semi-solid temperature during welding. Voids can be observed. This may be due to the solidification shrinkage and air trapped.

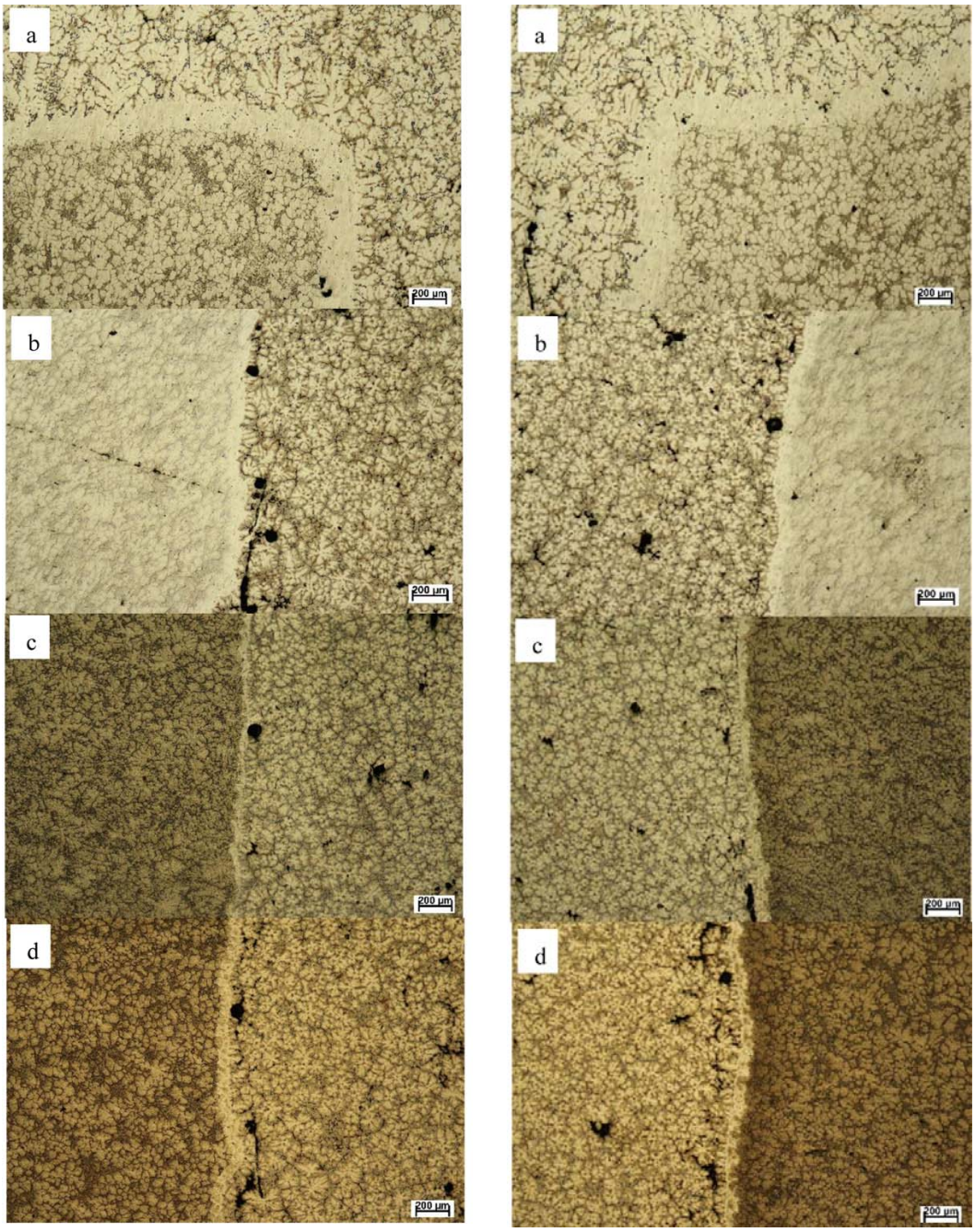

Figure 5. Microstructure of the interface area in semi-solid state joining at various welding speeds: (a) 15 mm/min, (b) 25 mm/min, (c) 40 mm/min and (d) 70 mm/min.

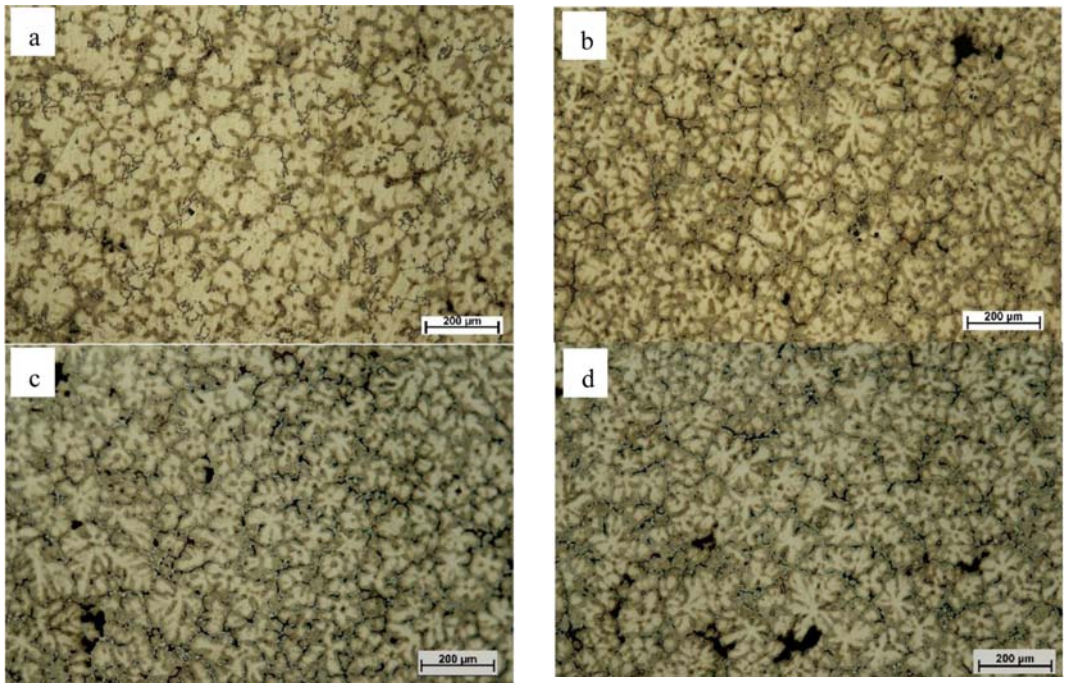

Figure 6. Microstructure of the weld metal (ZA27) in semi-solid state joining at various welding speed: (a) 15 mm/min, (b) 25 mm/min, (c) 40 mm/min and (d) 70 mm/min.

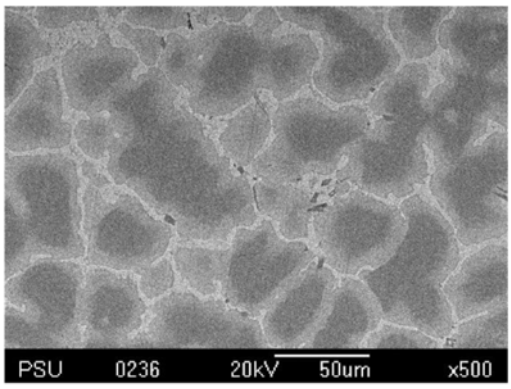

Figure 7. Back-scattered SEM image of the weld metal zone (ZA27) temperature of 450 °C.

3.2 SEM Analysis

Figure 7 shows the SEM image of the ZA27 filler heated at 450°C and quenched in water to observe its microstructure at the semi-solid temperature. The dark gray area is aluminum rich phase and the bright grain boundary is zinc rich phase.

Figure 8 shows SEM image and EDS mappings observed at the interface (advancing side) of the specimen welding under the best condition using a rotation speed of 1,750 rpm and a welding speed of 15 mm/min. As illustrated on the SEM image, left side is the base metal and right side is the weld metal. This is confirmed clearly by the elemental distribution mappings that Al and Si are mainly presented in the base metal (left side) while Zn is greatly available at the filler metal zone (right side). However, it is noticed that some Si were spread into the filler zone, whereas some Zn were propagated to the base metal region. These phenomena could be occurred during stirring process. Figure 9 shows SEM image and EDS mappings observed on the weld metal using the best synthesis condition. It can be seen that the α-Al phase exhibited a clear globular structure as a result of stirring. It is suggested that the joint consisted of equiaxed α-Al grains surrounded by η-Zn phase at the grain

boundary. The α-Al grain size is around 50-60 µm. The Al and Zn distribution on the weld region were noticed here. The amount of Zn, nevertheless, was highest at the centerline of welding. This may be due to the effect of high rotation speed (1750 rpm) used driving the Zn phase, that was all homogeneously distributed around the Al grain boundary, to the particular welding centerline.

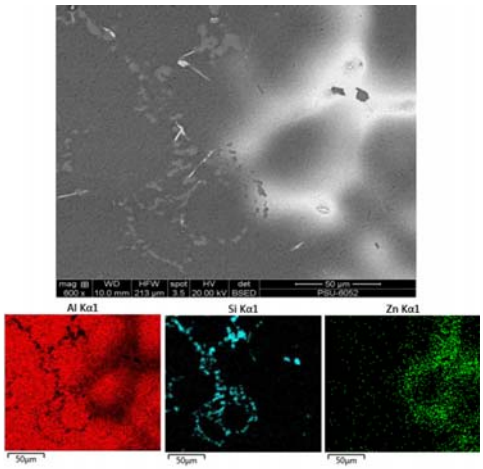

Figure 8. Back-scattered SEM image and EDS mappings of the interface area (advancing side) welding at the rotation speed of 1,750 rpm and the welding speed of 15 mm/min.

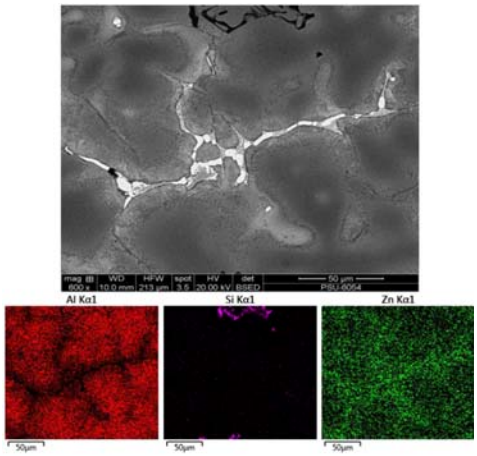

Figure 9. Back-scattered SEM image and EDS mappings of the weld metal area welding at the rotation speed of 1,750 rpm and the welding speed of 15 mm/min.

3.3 Mechanical Properties of The Joints

Transverse tensile strength, yield strength and elongation of the joints are presented in Figure 10. When welding speed increased, tensile strength of the joint reduced continuously. In addition, at the welding speed of 15 mm/min and the rotation speed of 1,750 rpm, the average tensile strength and yield strength reached the maximum value of 113.8 and 69 MPa, respectively. The similar tendency was observed on elongation analysis. This is related to the voids presented near the interface. The fracture appearance was at interface (retreating side). This is the porosity area.

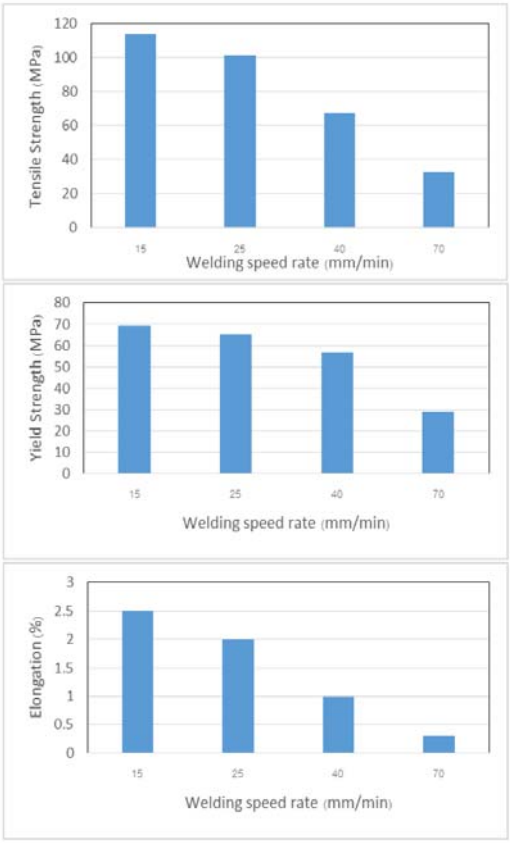

Figure 10. Values of tensile strength, yield strength and elongation of the joints of the semi-solid state joining.

Figure 11 shows the hardness values of the joint focused on 2 areas; interface and weld metal. It was found that the highest hardness was gained from the lowest welding speed (15 mm/min). The averaged hardness values at the interface, the weld metal and the base metal were 139, 149.5 and 67.3 HV, respectively. It can be seen that the weld metal possessed the highest hardness. This may be because of its globular microstructure.

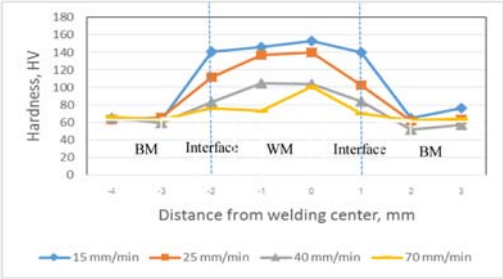

Figure 11. Values of hardness on transverse cross section of the joints of the semi-solid state joining.

4. CONCLUSIONS

The semi-solid state joining of SSM aluminum alloys using brazing ZA27 has been successfully performed under a normal atmosphere. The results can be summarized as follows:

1. The weld metal zone exhibits the globular microstructure.

2. SEM image and EDS mappings observed on the weld metal using the best synthesis condition. It can be seen that the α-Al phase exhibited a clear globular structure as a result of stirring. It is suggested that the joint consisted of equiaxed α-Al grains surrounded by η-Zn phase at the grain boundary. The α-Al grain size is around 50-60 μm.

3. Increase in welding speed promotes the formation of voids along the interface adjacent to the filler.

4. At the welding speed of 15 mm/min and stirring rate of 1,750 rpm, the average tensile strength, yield strength and elongation of the joints reached the maximum values of 113.8 MPa, 69 MPa and 2.5 %, respectively.

ACKNOWLEDGEMENTS

The work was supported by the Higher Education Research Promotion and National Research University Project of Thailand, Office of the Higher Education Commission. Researchers thank the Department of Mining and Materials Engineering, Faculty of Engineering, Prince of Songkla University in Thailand.

REFERENCES

[1] Wannasin J., Thanabumrungkul S., *Songklanakarin J. Sci. Technol.,* 2008; **30(2)**: 215-220.

[2] Romadorn Burapa, Rungsinee Canyook, Jessada Wannasin.,*PSU-E Engineering Conference* (*PEC*-5)., 2009; 21-22.

[3] Prapas Muangjunburee., *Proceeding of Prince of Sonkla University Engineering Conference, PEC-6.,* 2008; 599-602.

[4] Akhter R., Ivanchev L. and Bruger H.P., *Materials Science and Engineering. Forum Vol.447.,* 2007; 192-196.

[5] Worapong Boonchouytan, Thanate Ratanawilai, Prapas Muangjunburee., *Advanced Materials Research Vols. 488-489.,* 2012: 328-334.

[6] Narimannezhad A., Aashuri H., Kokabi A.H., et al., *J Mater Process Technol.,* 2009; **209**: 4112-4121.

[7] Alvani S.M.J., Aashuri H., Kokabi A., et al*., Trans Nonferrous Met Soc China.,* 2010; **209**: 1792-1798.

[8] Huibin Xu., Quanxiang Luo., Bofang Zhou., et al., *Materials and Design.,* 2012; **34**: 452-458.

[9] Huibin Xu., Bcfang Zhou., Changhua, et al., *J. Mater. Sci. Technol.,* 2012; **28(12)**: 1163-1168.

[10] http://www.dynacast.com/die-casting/zinc-die-casting/za27

[11] Aashuri H., *Mater. Sci. Eng.,* 2005; **A391**: 77-85.